

EFFECT OF WATER CONTENT ON THE MECHANICAL BEHAVIOR AND ENERGY EVOLUTION OF SOFT ROCK UNDER UNIAXIAL COMPRESSION

Yang LIU^{1*}, Hongjun LI²

¹ School of Architectural Engineering, Sichuan Polytechnic University, Deyang, 618000, China

² China Anergy Group Third Engineering Bureau Co. Ltd., Chengdu 610036, China

*corresponding author, 201911601006@stu.hebut.edu.cn

To investigate the influence of water content on the mechanical behavior and the energy evolution law of soft rocks, uniaxial compression tests were carried out on soft rock samples prepared from rock-like materials with different water contents. The test results suggest that under uniaxial compression conditions, as the water content of the soft rock samples increases, the failure pattern is single axial splitting failure (ASF), axial splitting local expansion mixed failure and single local expansion failure (LEF), respectively. The uniaxial compressive strength (UCS) exhibits an exponential decrease, while the elastic modulus displays a linear decline. Additionally, the axial peak strain initially declines and then increases. The total and elastic energies increase exponentially, whereas the dissipated energy decreases linearly. Elastic energy as a percentage of total energy decreases, while dissipated energy as a percentage of total energy increases.

Keywords: soft rock; water content; mechanical behavior; energy evolution.



Articles in JTAM are published under Creative Commons Attribution 4.0 International.
Unported License <https://creativecommons.org/licenses/by/4.0/deed.en>.
By submitting an article for publication, the authors consent to the grant of the said license.

1. Introduction

Soft rocks are widely distributed in nature and are frequently found in all types of geological engineering. In accordance with the definition set forth by the International Society of Rock Mechanics (ISRM), soft rocks are classified as a group of rocks with a uniaxial compressive strength (UCS) falling between 0.5 MPa and 25 MPa (Cripps & Moon, 1990), such as mudstone, muddy siltstone, muddy mineral rock and so on. Soft rocks usually have mechanical and physical characteristics such as low strength, loose structure (low density), water swelling by absorption, and disintegration by dehydration. The mineral composition (comprising a significant proportion of hydrophilic minerals) and structural characteristics of soft rocks have been demonstrated to be influenced by water, which plays an important role in determining their mechanical behavior (Vásárhelyi, 2005; Vásárhelyi & Ván, 2006; Ciantia *et al.*, 2015; Cherblanc *et al.*, 2016). Nevertheless, water is frequently present during construction in a multitude of soft rock strata. Such circumstances may be exemplified by open-pit mining operations conducted under conditions of heavy precipitation, the construction of reservoir slopes, and the excavation of tunnels in rock strata with the elevated water content.

The influence of water on the mechanical behavior of soft rocks has been the subject of study by a number of scholars. However, the majority of these studies have concentrated on saturated soft rocks and the effects of dry-wet cycles on them. He *et al.* (2021) studied the damping behavior of soft rock by cyclic loading tests, they found that as the stress amplitude decreased, the moisture content had a lesser effect on the dynamic shear modulus and a greater effect on the damping parameters. Li *et al.* (2023) studied the mechanical deformation characteristics of the clay-red stratum soft rock mixture before and after wetting by using a large-scale triaxial test.

They found that wetting led to a decrease in the shear strength and critical strain of the samples, and a decrease in the critical internal friction angle and tangent modulus, which intensified the crushing of the rock blocks. Liu *et al.* (2024) studied the micro-pore dissolution mechanism and macroscopic mechanical behavior of red-bed soft rock by the dry-wet cycle method and a series of uniaxial compression tests. Their results showed that with an increase in the number of dry-wet cycles, the macroscopic failure mode changes from brittle splitting failure to ductile conical failure under the action of the axial load. Zhang *et al.* (2024) studied the mechanism and influence on red-bed soft rock disintegration durability of particle roughness based on the experiment and fractal theory, they found that the roughness decreases with increasing dry-wet cycles, but increases with decreasing particle size. Yu *et al.* (2023) studied the disintegration mechanism of the soft rock due to water intrusion based on the discrete element method, their results showed that the breaking force and the residual strength coefficient of the complete sample exhibit an exponential attenuation relationship with the increase of water content. Fu *et al.* (2021) used the nuclear magnetic resonance (NMR) technology to visualize and quantify the dynamics of water infiltration and distribution in initially unsaturated sandstone. They found that the strength and Young's modulus of sandstones decrease as a function of increasing water saturation.

The deformation and damage evolution processes in rock are accompanied by energy conversion, including the accumulation, dissipation, and release of energy (Xie *et al.*, 2009; Huang & Li, 2014; Chen *et al.*, 2017). Currently, the energy evolution during rock damage can be obtained from the calculation of its stress-strain curve or from the analysis of the collected signals of acoustic emission. Gao *et al.* (2020) investigated the energy evolution characteristics, and identified the damage and crack propagation thresholds based on the uniaxial loading-unloading experiments for five types of rocks. They found that the evolution characteristics of the strain energy rates can be easily identified by the crack propagation thresholds. Gong *et al.* (2021) proposed a theoretical method for characterising the damage of intact rocks under uniaxial compression conditions based on the linear energy dissipation law and the energy dissipation coefficient, they found that with the linear energy storage law serving as a theoretical basis, the peak dissipated strain energy in a rock damage expression under uniaxial compression can be accurately calculated. Meng *et al.* (2023) studied the effects of cyclic loading and unloading rates on the energy evolution of rocks with different lithology, they found that the energy of all rock samples increased nonlinearly with the increase in axial stress, and the elastic energy increased gradually first and subsequently rapidly with the increase in the axial stress. Xi *et al.* (2023) studied the transient process of the mechanical response and energy conversion of rocks with different lithologies under impact loading, their results showed that the fracture energy of the rock increases as the strain rate increases.

The objective of this study was to investigate the effect of water on the mechanical behavior and energy evolution of soft rock. To this end, uniaxial compression tests were performed on soft rock samples with the different water content. A correlation was identified between mechanical parameters, including UCS, elastic modulus and peak strain, and the water content of the soft rock samples. The evolution laws of total energy, elastic energy and dissipated energy in soft rock with varying water contents were investigated. The findings of this study can provide the theoretical guidance on the construction and maintenance of projects in water-bearing soft rock strata.

2. Test methods

2.1. Sample preparation

Despite the prevalence of soft rocks in nature, the preparation of standard cylindrical samples with a specific water content remains a challenging endeavour. This is due to the fact that natural soft rocks lose their structural integrity rapidly upon contact with water, leading to

the formation of fissures when dehydrated. Rock-like materials have been widely used in rock mechanical behavior tests as well as model tests (Luo *et al.*, 2023; Liu *et al.*, 2023a; 2023b). For example, Liu *et al.* (2023a) investigated the compression characteristics of fractured soft rock and its Mohr–Coulomb criterion by means of soft rock samples prepared from rock-like materials. Therefore, in this study, rock-like materials were used to prepare standard soft rock samples with the specific water content. As shown in Fig. 1, the rock-like material consists of quartz sand, kaolin, gypsum, 42.5 normal silicate cement, barite powder, and water. Barite powder and quartz sand were used as the coarse aggregate, and gypsum, kaolin, and cement were used as the binder. The barite powder can effectively improve the sample density, gypsum can effectively prevent the rapid solidification of the mixed mortar, and kaolin can appropriately increase the plasticity of the sample. In order to prepare soft rock samples whose mechanical properties are highly similar to those of the real soft rock (mudstone), a lot of attempts were made on the mass ratio of the rock-like materials in the preliminary stage. By constantly adjusting the proportion of rock-like materials, the soft rock samples with mechanical properties highly similar to those of the real soft rock (mudstone) were finally obtained. The mass ratio of the rock-like materials used to prepare the soft rock samples is shown in Table 1. According to the ISRM (Fairhurst & Hudson 1999), the standard cylinder soft rock samples of 50 mm × 100 mm (diameter × height) are prepared and the basic mechanical parameters of the prepared soft rock samples are shown in Table 2.

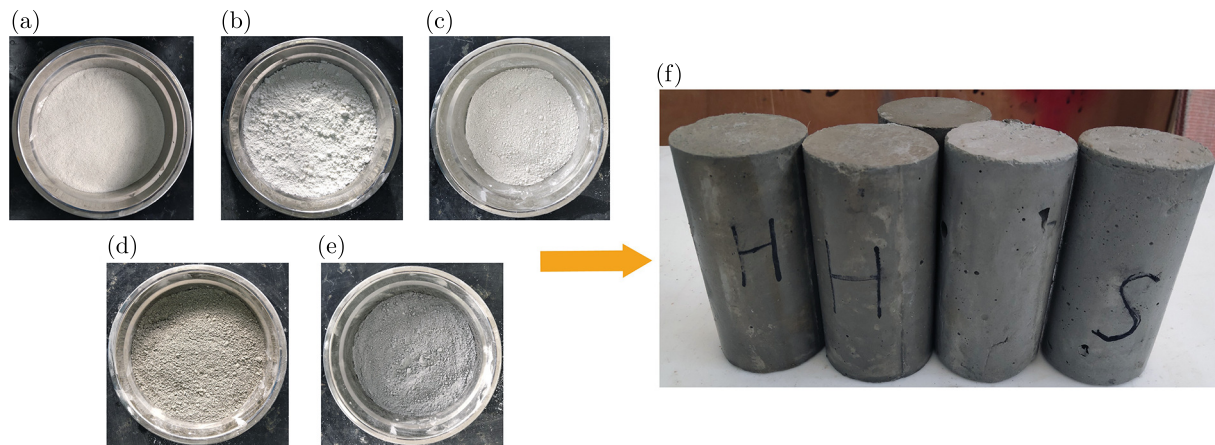


Fig. 1. Rock-like materials for the preparation of soft rock and partially prepared soft rock samples: (a) quartz sand; (b) kaolin; (c) gypsum; (d) cement; (e) barite powder.

Table 1. Material ratios for the preparation of the soft rock.

Type	Quartz sand	Barite powder	Cement	Gypsum	Kaolin	Water-binder ratio
Ratio	0.75	0.25	1.5	0.45	0.35	0.40

Table 2. Basic mechanical parameters of the prepared soft rock samples (dry).

Mechanical parameters	Uniaxial compression strength [MPa]	Tensile strength [MPa]	Elasticity modulus [GPa]	Poisson's ratio	Cohesive force [kN]	Internal friction angle [°]
Value	18.68	2.14	3.68	0.22	2.42	15.23

2.2. Test equipment

Uniaxial compression tests were carried out by the MTS-793 rock mechanics testing machine (Fig. 2) with an axial force loading range of -200 kN to $+200$ kN, and the accuracy of axial force data collection is 0.001 kN, the accuracy of axial deformation data collection is 0.001 mm.



Fig. 2. MTS-793 rock mechanics testing machine.

2.3. Test procedure

The specific procedure of uniaxial compression test for soft rock with different water content was as follows:

Step 1: The prepared soft rock samples were subjected to drying in an oven at a temperature of 110 °C for a period of 24 hours. Following this, the mass of the samples was measured, resulting in a value designated M_d . Subsequently, the dried samples were saturated with water under vacuum after standing at room temperature, resulting in a saturated water content of 14 % for the soft rock samples.

Step 2: The saturated soft rock samples were placed in an oven at 60 °C and removed at 2-minute intervals to determine their mass, M_w . Therefore, the real-time water content of the soft rock samples can be calculated by Eq. (2.1). When the water content of the soft rock samples was determined, a thin and uniform layer of silicone oil was applied to the surface to prevent the moisture from changing over a short period of time.

$$\omega_t = \frac{M_w - M_d}{M_d} \times 100 \%, \quad (2.1)$$

where ω_t is the water content of the soft rock samples, M_w is the mass of water-bearing soft rock samples, M_d is mass of dried soft rock samples.

Step 3: Soft rock samples with specified water contents were loaded into the MTS-793 rock mechanics testing machine, and axial load was applied at a static loading rate of 0.01 mm/min until the samples failed. To guarantee the precision of the test data, three samples of soft rock were tested for each water content level.

3. Test results

3.1. Stress-strain curves

The uniaxial compressive stress-strain curves of soft rock samples with different water contents are shown in Fig. 3. The water content has a significant effect on the trend of stress-strain curves of soft rock samples. The evolution of uniaxial compressive stress-strain curves of soft rock samples can be generally divided into four stages: the plastic deformation stage, the elastic

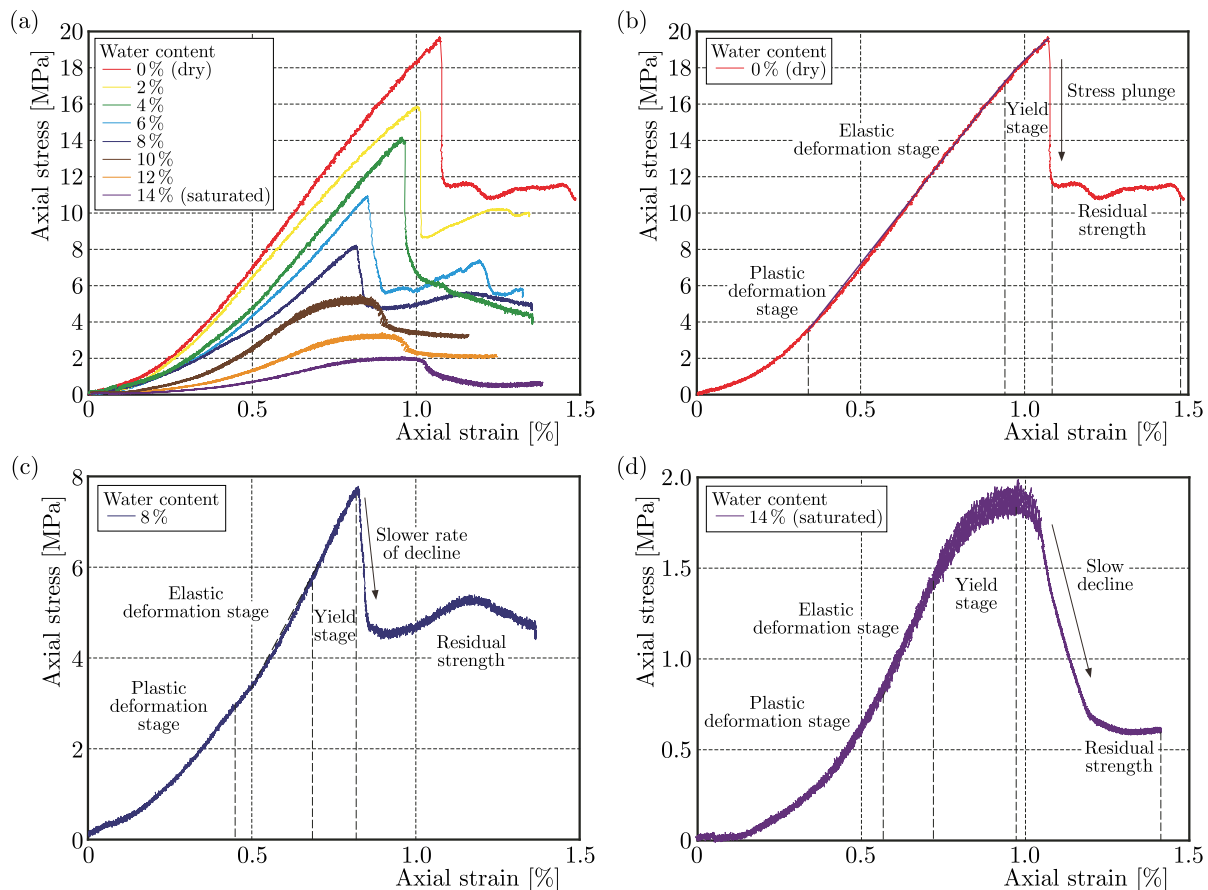


Fig. 3. Uniaxial compressive stress-strain curves of soft rock samples with different water contents.

deformation stage, the yielding stage and the residual stress stage (Fig. 3a). As the water content of the soft rock samples increases, the proportions of the plastic deformation and yielding stages of the stress-strain curve increase, while the proportion of the elastic deformation stage decreases (Figs. 3b–3d). Furthermore, as the water content of the soft rock samples increases, after the peak axial stress of failure is reached, the rate of decrease of axial stress decreases, but the percentage of decrease increases. For example, when the water content of the soft rock sample is 0% (dry), after reaching the peak axial stress, its axial stress decreases instantaneously and sharply. The axial stress decreased from 19.64 MPa to 11.61 MPa, a reduction of 40.87% (Fig. 3b). When the water content of the soft rock sample is 14% (saturated), the axial stress decreases slowly after the peak axial stress is reached. The axial stress decreased from 1.94 MPa to 0.69 MPa, a reduction of 64.35% (Fig. 3d).

3.2. Peak stress, elastic modulus and peak strain

The relationship between peak stress, elastic modulus, peak strain and water content of soft rock is shown in Fig. 4. The water content has a significant effect on the peak stress (UCS), elastic modulus and axial peak strain of soft rock. As shown in Fig. 4a, the uniaxial compressive strength of soft rock samples decreases with increasing the water content and their relationship can be fitted well by an exponential function. The average UCS was 18.99 MPa when the water content of the soft rock samples was 0% (dry), and 1.95 MPa when the water content of the soft rock samples was 14% (saturated). When the water content of the soft rock samples increased from 0% (dry) to 8%, the UCS decreased by an average of 21.64% for every 2% increase in the water content, while when the water content of the soft rock samples increased from 8% (dry) to 14%, the uniaxial compressive strength decreased by an average of 29.01% for every 2%

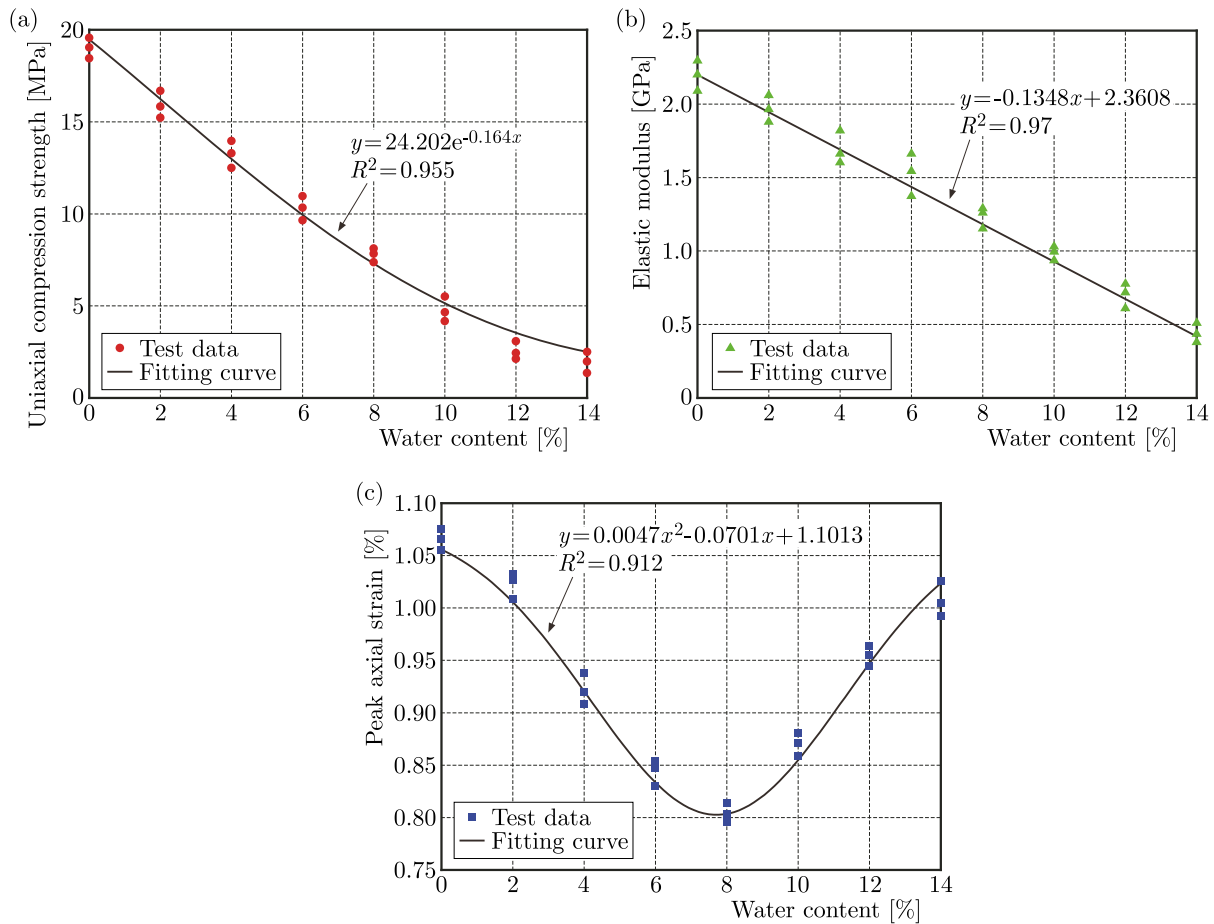


Fig. 4. Relationship between peak stress, elastic modulus, peak strain and water content of soft rock.

increase in the water content. The decrease in UCS increased significantly with the increase in water content of the soft rock samples. As shown in Fig. 4b, the elastic modulus of soft rock samples decreases linearly with increasing water content. With each 2% increase in the water content of the soft rock samples, the elastic modulus decreased on average by 0.25 GPa. As shown in Fig. 4c, the peak axial strain of soft rock samples first decreases and then increases with increasing water content. The relationship between peak axial strain and the water content can be fitted well by a quadratic function. When the water content of a soft rock samples is low, it has a strong load-bearing capacity, its peak axial strain is larger, and it is mainly elastic deformation. However, as the water content of the soft rock samples increases, the bearing capacity decreases, but the deformation increases and is mainly plastic.

3.3. Ultimate failure pattern

Ultimate failure patterns of soft rock samples with different water contents under uniaxial compression tests are shown in Fig. 5. With the gradual increase of the water content of the soft rock samples, their ultimate failure patterns under uniaxial compression conditions changed from single axial splitting failure (ASF) to mixed ASF and the local expansion failure (LEF) and then to single LEF. As shown in Figs. 5a and 5b, when the water content of the soft rock samples is 0% (dry) and 2%, the initial cracks sprout at the end of the sample and then developed towards the other end, its width gradually becomes narrower, and the failure pattern is dominated by ASF. As shown in Figs. 5c–5f, when the water content of the soft rock samples was 4%, 6%, 8%, and 10%, LEF occurred at one end of the sample (about one-third of the total length of the sample), while the other end of the sample remained ASF. The LEF is manifested

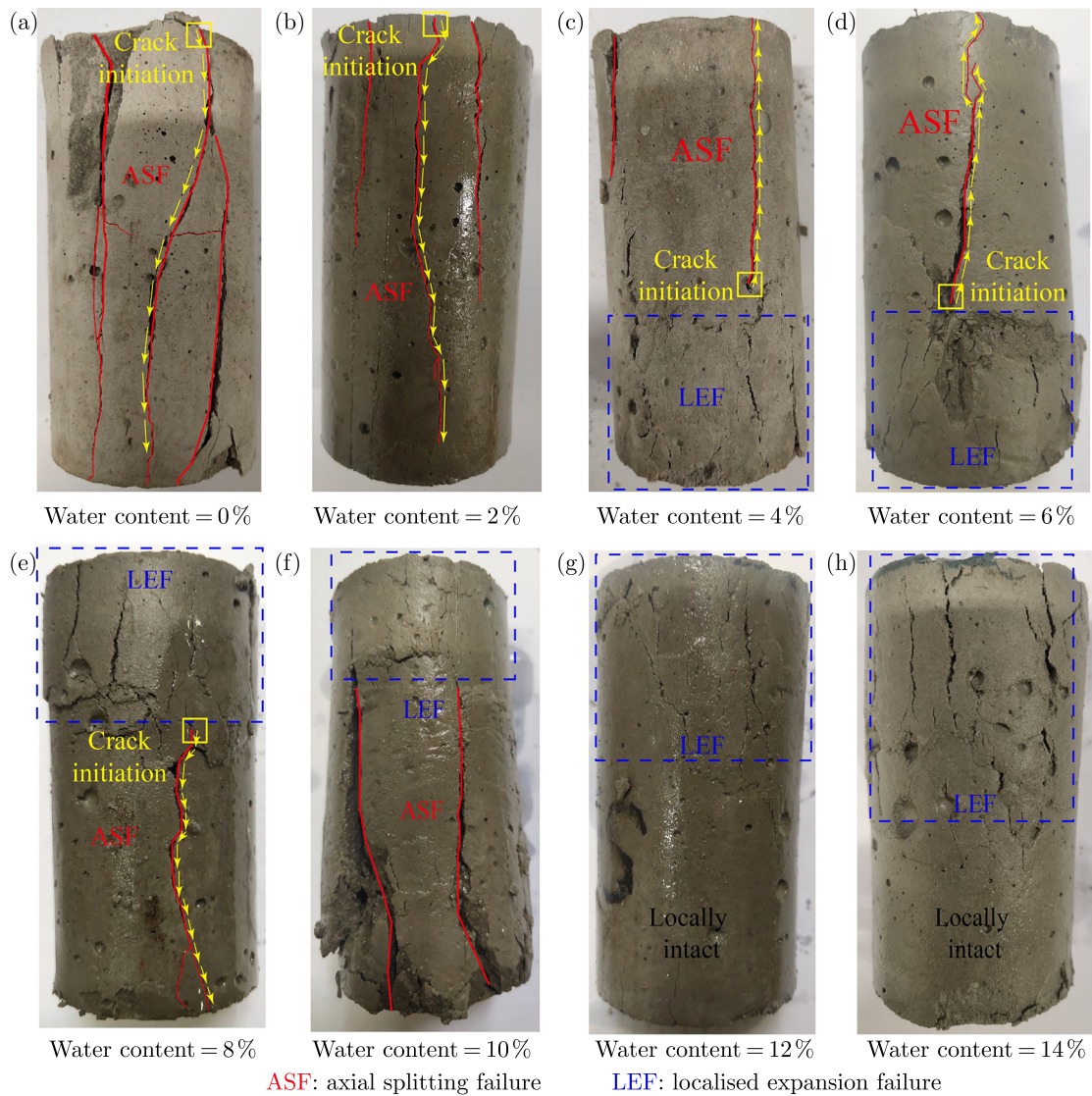


Fig. 5. Ultimate failure patterns of soft rock samples with different water contents.

as a circumferential increase in the volume of the sample and is accompanied by a small number of micro-cracks. Meanwhile, the initial cracks of ASF sprout at the interface of local expansion failure and then develop towards the other end of the sample. As shown in Figs. 5g and 5h, when the water content of the soft rock samples is 12% and 14%, the ultimate failure pattern of the samples is dominated by local expansion failure. In addition, the extent of LEF of the soft rock samples increased from one-third to two-thirds of their total length as the water content increased.

4. Energy conversion

4.1. Calculation of energy

The energy composition of the soft rock sample under uniaxial compression is shown schematically in Fig. 6. The total input energy (U) of a rock sample under uniaxial compression consists of the elastic energy (U_e) and the dissipated energy (U_d). The total input energy (U) is the work done on the rock sample by the external load applied by the rock mechanics testing machine, which can be obtained by calculating the total area of the stress-strain curve (given by the area

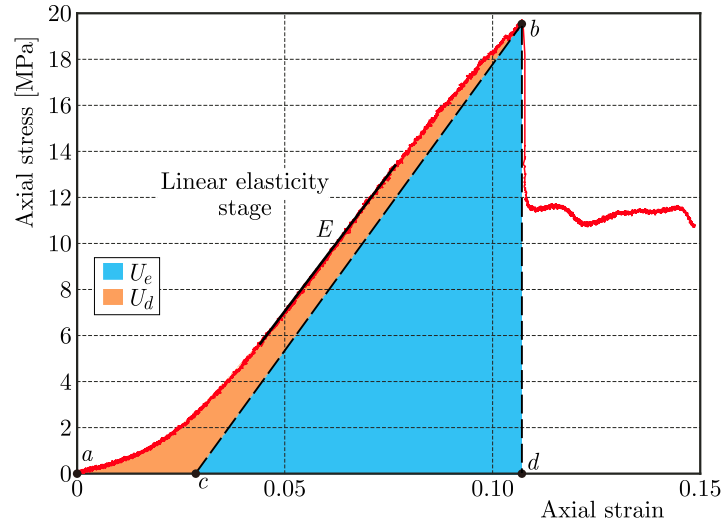


Fig. 6. Stress-strain curve and strain energy.

of figure described by points abd , see Fig. 6). The elastic energy (U_e) is the energy stored by the elastic deformation of the rock sample during compression deformation (given by the area of the figure described by points cbd , see Fig. 6), and the dissipated energy (U_d) is the energy dissipated by the plastic deformation of the rock sample during compression deformation (given by the area of figure described by points abc , see Fig. 6). Therefore, the total energy, elastic energy and dissipated energy are calculated as shown in Eq. (4.1), respectively (Xie *et al.*, 2009; Huang & Li, 2014; Chen *et al.*, 2017):

$$U = \int_a^d \sigma_a d\varepsilon_a, \quad U_e = \frac{1}{2E} \sigma_a^2, \quad U_d = U - \frac{1}{2E} \sigma_a^2, \quad (4.1)$$

where σ_a is the axial stress, ε_a is the axial strain, E is the elastic modulus.

4.2. Energy evolution

Energy evolution laws of soft rock samples with different water contents under uniaxial compression tests are shown in Fig. 7. The energy evolution process of a soft rock sample is closely related to its specific deformation pattern. The elastic and dissipated energies represent the elastic and plastic deformation of the soft rock sample, respectively. The total energy is defined as the total work done by the rock mechanics testing machine and therefore exhibits a rapid increase. In contrast, the evolutionary law of the elastic and dissipated energies is contingent upon the deformation pattern that occurs in the soft rock sample. In the absence of water in the soft rock sample (i.e., when it is dry), both the total and elastic energies evolve in a similar manner, exhibiting a rapid increase with increasing axial strain. However, the rate of increase in dissipated energy is slow with increasing axial strain (Fig. 7a). When the water content of the soft rock sample is 8%, the evolution trends of the total and elastic energies remain generally consistent and continue to increase rapidly as the axial strain increases. However, there is a notable discrepancy between the two energies, with the elastic energy displaying a greater increase than the total energy. Concurrently, the dissipated energy increases gradually initially and then remains constant with increasing axial strain (Fig. 7b). At a water content of 14% in the soft rock sample, the total energy increases rapidly with increasing axial strain. The elastic energy increases rapidly and then levels off, while the dissipation energy increases slowly and then rapidly (Fig. 7c).

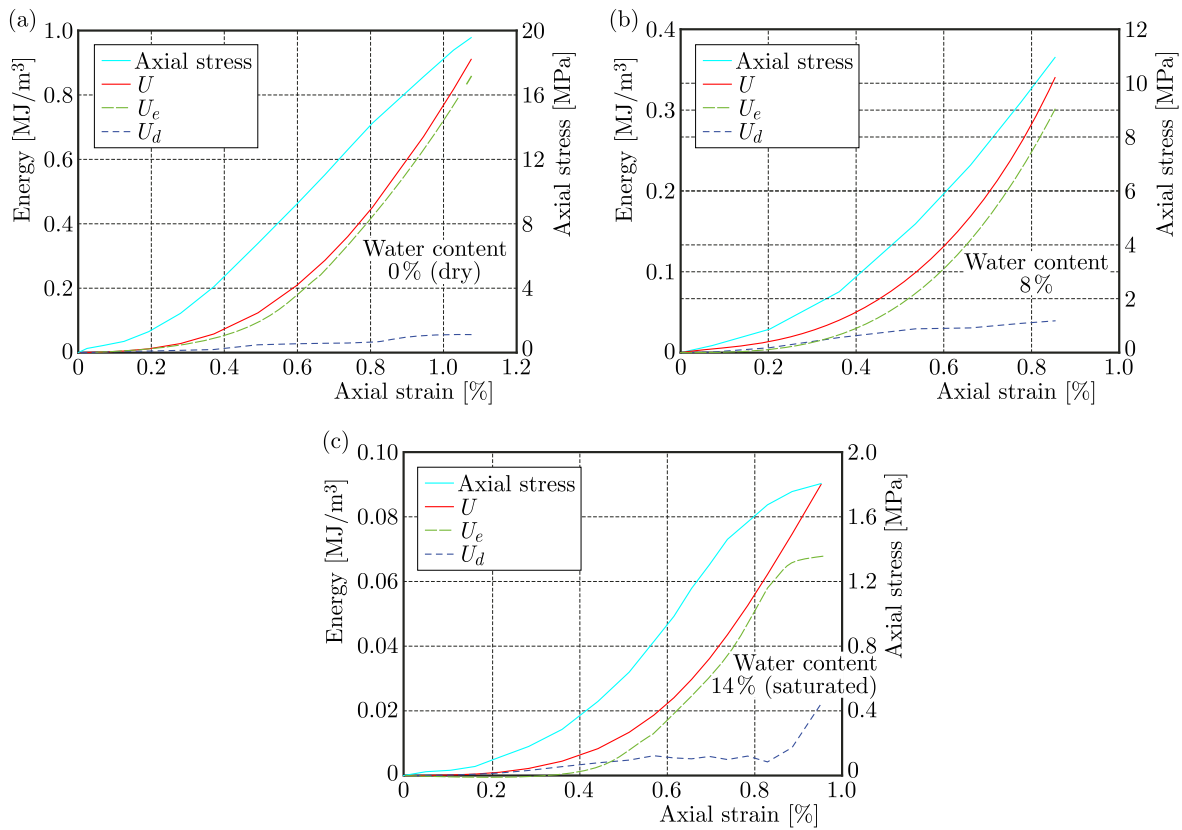


Fig. 7. Energy evolution laws of soft rock samples with different water contents under uniaxial compression tests.

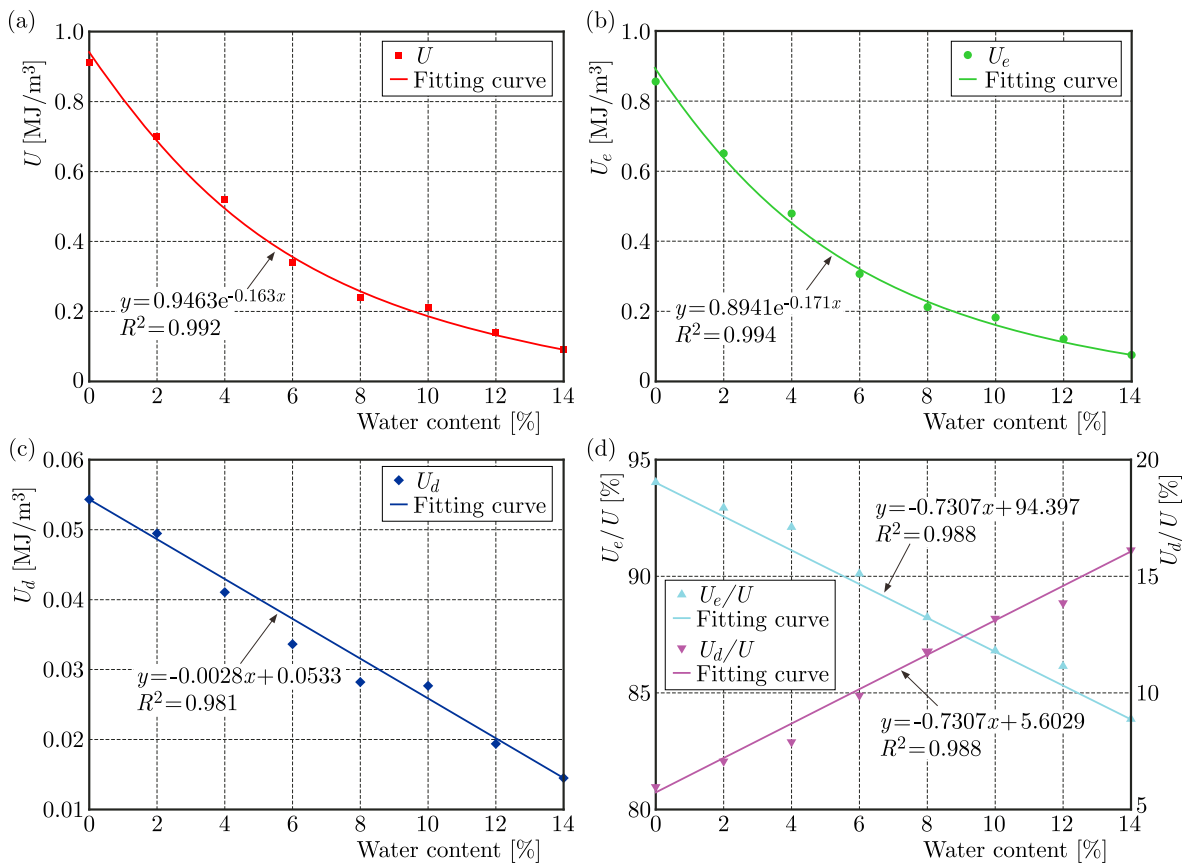


Fig. 8. Relationship between total energy, elastic energy, dissipated energy, and percentage water content.

4.3. Characteristics of energy at UCS

The relationship between total energy, elastic energy, dissipated energy and percentage water content at UCS for soft rock samples is shown in Fig. 8. It can be seen from Figs. 8a and 8b, with the increase of water content of soft rock samples, the total energy and elastic energy are gradually reduced, and the change rule can be well fitted by the exponential function. Meanwhile, as shown in Fig. 8c, the dissipated energy decreases linearly with the increase of water content of soft rock samples. Moreover, as illustrated in Fig. 8d, the proportion of elastic energy in the total energy tends to decrease linearly with increasing water content in the soft rock samples, while the dissipated energy proportion shows a linear increase. This suggests that as the water content of the soft rock sample increases, there is an accompanying increase in plastic deformation and a decrease in elastic deformation during the process of compressive deformation. The dissipation of input energy occurs predominantly through plastic deformation, with a lesser degree of energy storage occurring in the elastic deformation phase.

5. Discussion

Numerous studies have shown that the water content leads to significant changes in the mechanical behavior of soft rocks mainly due to the physical-chemical effect and the mechanical effect (Liu *et al.*, 2021; Wasantha & Ranjith, 2014). The micrographs of the soft rock under dry and saturated conditions are presented in Fig. 9. When the soft rock is in a dry state, the surface of the sample displays a structurally compact appearance with a reduced number of micro-cracks. However, when the soft rock is in a saturated state, its structure becomes looser, and a considerable number of micro-cracks are evident. The increased plasticity of the soft rock samples during compressive deformation is attributed to the loosened structure and the elevated number of micro-cracks. This provides an explanation as to why the dissipated energy as a percentage of the total energy in uniaxial compression conditions of soft rock increases with increasing water content.

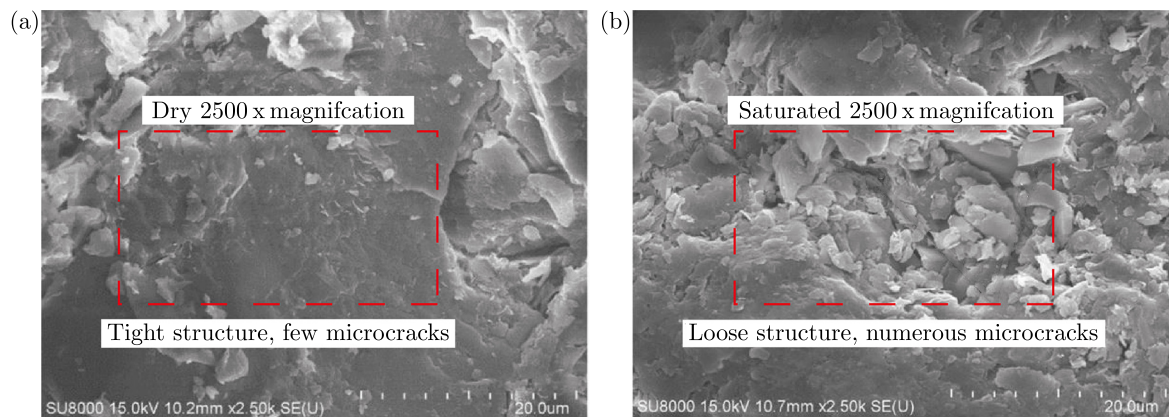


Fig. 9. Scanning electron microscopy images of dry and saturated soft rock (Liu *et al.*, 2021).

6. Conclusion

By conducting uniaxial compression tests on soft rock samples prepared from rock-like materials with the different water content, this study investigated the effect of water content on the strength, deformation, failure pattern, and energy evolution law of soft rock samples. The main conclusions are summarized as follows:

- 1) The UCS exhibits an exponential function-decreasing trend, while the elastic modulus demonstrates a linear decrease as the water content of the soft rock samples increases.

The peak axial strain initially exhibits a decline, followed by an uptick. Its correlation with the water content can be effectively captured by a quadratic function.

- 2) The water content has a significant effect on the failure pattern of soft rock samples under the uniaxial compression condition. With the increase of water content, the failure pattern is single ASF, axial splitting local expansion mixed failure and single LEF, respectively.
- 3) As the water content of the soft rock sample increases, both the total input energy and the elastic energy exhibit an exponential function that demonstrates a decreasing trend, while the dissipated energy displays a linear decreasing trend. Furthermore, as the water content of the soft rock samples increases, the proportion of elastic energy in the total energy decreases linearly, while the proportion of dissipated energy in the total energy increases linearly.

Acknowledgments

This work is supported by the Graduate Student Innovation Foundation of Hebei Province (grants no. CXZZBS2022034).

References

1. Chen, Z.Q., He, C., Wu, D., Xu, G.W., & Yang, W.B. (2017). Fracture evolution and energy mechanism of deep-buried carbonaceous slate. *Acta Geotechnica*, 12(6), 1243–1260. <https://doi.org/10.1007/s11440-017-0606-5>
2. Cherblanc, F., Berthonneau, J., Bromblet, P., & Huon, V. (2016). Influence of water content on the mechanical behaviour of limestone: role of the clay minerals content. *Rock Mechanics and Rock Engineering*, 49(6), 2033–2042. <https://doi.org/10.1007/s00603-015-0911-y>
3. Ciantia, M.O., Castellanza, R., Crosta, G.B., & Hueckel, T. (2015). Effects of mineral suspension and dissolution on strength and compressibility of soft carbonate rocks. *Engineering Geology*, 184, 1–18. <https://doi.org/10.1016/j.enggeo.2014.10.024>
4. Cripps, J.C. & Moon, C.F. (1990). *The Engineering Geology of Weak Rock*, Leeds University Press.
5. Fairhurst, C.E. & Hudson, J.A. (1999). Draft ISRM suggested method for the complete stress-strain curve for intact rock in uniaxial compression. *International Journal of Rock Mechanics and Mining Sciences*, 36(3), 279–289. [https://doi.org/10.1016/S0148-9062\(99\)00006-6](https://doi.org/10.1016/S0148-9062(99)00006-6)
6. Fu, T.F., Xu, T., Heap, M.J., Meredith, P.G., Yang, T.H., Mitchell, T.M., & Nara, Y. (2021). Analysis of capillary water imbibition in sandstone via a combination of nuclear magnetic resonance imaging and numerical DEM modeling. *Engineering Geology*, 285, Article 106070. <https://doi.org/10.1016/j.enggeo.2021.106070>
7. Gao, L., Gao, F., Zhang, Z.Z., & Xing, Y. (2020). Research on the energy evolution characteristics and the failure intensity of rocks. *International Journal of Mining Science and Technology*, 30(5), 705–713. <https://doi.org/10.1016/j.ijmst.2020.06.006>
8. Gong, F.Q., Zhang, P.L., Luo, S., Li, J.C., & Huang, D. (2021). Theoretical damage characterisation and damage evolution process of intact rocks based on linear energy dissipation law under uniaxial compression. *International Journal of Rock Mechanics and Mining Sciences*, 146, Article 104858. <https://doi.org/10.1016/j.ijrmms.2021.104858>
9. He, M.M., Zhang, Z.Q., & Li, N. (2021). Experimental investigation and empirical model to determine the damping and shear stiffness properties of soft rock under multistage cyclic loading. *Soil Dynamics and Earthquake Engineering*, 147, Article 106818. <https://doi.org/10.1016/j.soildyn.2021.106818>
10. Huang, D. & Li, Y.R. (2014). Conversion of strain energy in Triaxial Unloading Tests on Marble. *International Journal of Rock Mechanics & Mining Sciences*, 66, 160–168. <https://doi.org/10.1016/j.ijrmms.2013.12.001>

11. Li, S.Q., Yang, Z.P., Gao, Y.H., Liu, H., Liu, X.R., & Jin, X.G. (2023). Wetting deformation characteristics of soil–rock mixture considering the water-disintegration of red stratum soft rock. *Acta Geotechnica*, 19(7), 4381–4397. <https://doi.org/10.1007/s11440-023-02162-2>
12. Liu, C.D., Cheng, Y., Jiao, Y.Y., Zhang, G.H., Zhang, W.S., Ou, G.Z., & Tan, F. (2021). Experimental study on the effect of water on mechanical properties of swelling mudstone. *Engineering Geology*, 295, Article 106448. <https://doi.org/10.1016/j.enggeo.2021.106448>
13. Liu, H.D., Liu, J.J., Zhang, S.Y., Feng, L.Y., & Qiu, L. (2023a). Experimental study on compression characteristics of fractured soft rock and its Mohr-Coulomb criterion. *Theoretical and Applied Fracture Mechanics*, 125, 103820. <https://doi.org/10.1016/j.tafmec.2023.103820>
14. Liu, X.C., Huang, F., Zheng, A.C., & Hu, X.T. (2024). Micro-dissolution mechanism and macro-mechanical behavior of red-bed soft rock under dry-wet cycle. *Materials Letters*, 362, Article 136220. <https://doi.org/10.1016/j.matlet.2024.136220>
15. Liu, Y., Huang, D., Peng, J.B., & Guo, Y.Q. (2023b). Analysis of the effect of rock layer structure on the toppling failure evolution of soft-hard interbedded anti-dip slopes. *Engineering Failure Analysis*, 145, Article 107005. <https://doi.org/10.1016/j.engfailanal.2022.107005>
16. Luo, P.K., Li, D.Y., Ma, J.Y., Zhou, A.H., & Zhang, C.X. (2023). Experimental investigation on mechanical properties and deformation mechanism of soft-hard interbedded rock-like material based on digital image correlation. *Journal of Materials Research and Technology*, 24, 1922–1938. <https://doi.org/10.1016/j.jmrt.2023.03.145>
17. Meng, Q.B., Liu, J.F., Pu, H., Huang, B.X., Zhang, Z.Z., & Wu, J.Y. (2023). Effects of cyclic loading and unloading rates on the energy evolution of rocks with different lithology. *Geomechanics for Energy and the Environment*, 34, Article 100455. <https://doi.org/10.1016/j.gete.2023.100455>
18. Vásárhelyi, B. (2005). Statistical analysis of the influence of water content on the strength of the miocene limestone. *Rock Mechanics and Rock Engineering*, 38(1), 69–76. <https://doi.org/10.1007/s00603-004-0034-3>
19. Vásárhelyi, B. & Ván, P. (2006). Influence of water content on the strength of rock. *Engineering Geology*, 84(1–2), 70–74. <https://doi.org/10.1016/j.enggeo.2005.11.011>
20. Wasantha, P.L.P. & Ranjith, P.G. (2014). Water-weakening behavior of Hawkesbury sandstone in brittle regime. *Engineering Geology*, 178, 91–101. <https://doi.org/10.1016/j.enggeo.2014.05.015>
21. Xi, Y., Wang, H.Y., Li, J., Jiang, H.L., & Fan, L.F. (2023). Transient process of mechanical response and energy conversion of rocks with different lithologies under impact loading. *Geoenergy Science and Engineering*, 228, Article 211978. <https://doi.org/10.1016/j.geoen.2023.211978>
22. Xie, H.P., Li, L.Y., Peng, R.D., & Ju, Y. (2009). Energy analysis and criteria for structural failure of rocks. *Journal of Rock Mechanics and Geotechnical Engineering*, 1(1), 11–20. <https://doi.org/10.3724/SP.J.1235.2009.00011>
23. Yu, H.T., Liu, Z.B., Zhang, Y., Luo, T.Y., Tang, Y.S., Zhang, Q.S., & Wang, Y.T. (2023). The disintegration mechanism analysis of soft rock due to water intrusion based on discrete element method. *Computers & Geosciences*, 171, Article 105289. <https://doi.org/10.1016/j.cageo.2022.105289>
24. Zhang, G.D., Ling, S.X., Liao, Z.X., Xiao, C.J., & Wu, X.Y. (2024). Mechanism and influence on red-bed soft rock disintegration durability of particle roughness based on experiment and fractal theory. *Construction and Building Materials*, 419, Article 135504. <https://doi.org/10.1016/j.conbuildmat.2024.135504>

*Manuscript received June 4, 2024; accepted for publication March 7, 2025;
published online April 15, 2025.*